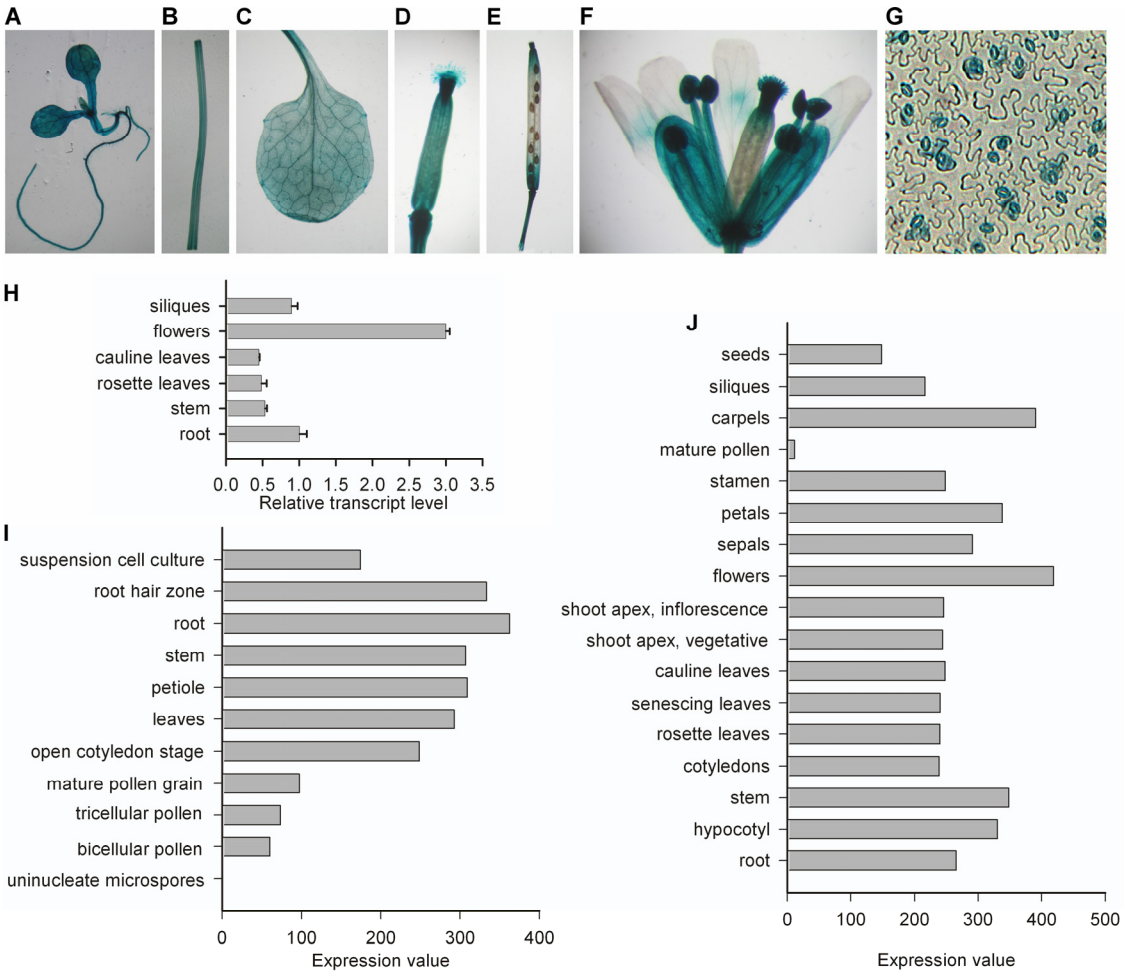

Supplemental Figure 1. Expression of *SCAB1* and its homologs in *Arabidopsis*.

(A-G) The *SCAB1* expression pattern as indicated by the promoter and GUS reporter fusion. *ProSCAB1:GUS* expression in seedlings **(A)**, stems **(B)**, leaves **(C)**, pistils **(D)**, siliques **(E)**, flowers **(F)**, and an epidermal peel **(G)**.

(H) Expression of *SCAB1* in various *Arabidopsis* tissues. Total RNA was extracted from the roots, stems, leaves, flowers, and siliques of 1-month-old WT plants. Real-time PCR was performed using *SCAB1*-specific primers. *Elongation factor 1α* (*EF*) was used as an internal control. The data given are the means ± SD (n = 3).

(I) Microarray analysis of *SCAB1* expression in pollen and other organs using data from the NASC (Honys and Twell, 2004).

(J) Microarray analysis of *SCAB1* expression in different organs using data from AtGeneExpress (Schmid et al., 2005).

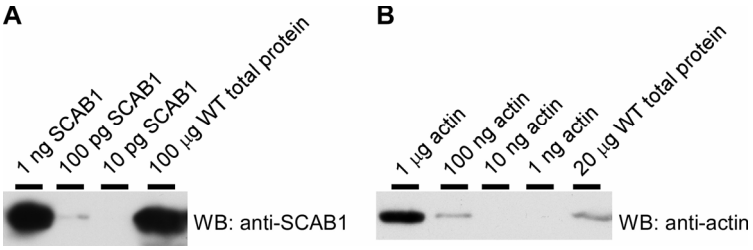

Supplemental Figure 2. Analyses of native SCAB1 concentration.
(A) Immunoblot analysis of the putative SCAB1 level in seedlings using anti-SCAB1 antibodies. Lanes 1-3 from left: 1 ng, 100 pg, and 10 pg of purified recombinant SCAB1; Lane 4, 100 μg of total soluble protein extracted from 1-day-old WT seedlings.
(B) Immunoblot analysis of the actin level in seedlings using anti-actin polyclonal antibodies. Lanes 1-4 from left: 1 μg, 100 ng, 10 ng, and 1 ng of purified actin; Lane 4, 20 μg of total soluble protein extracted from 1-day-old WT seedlings.

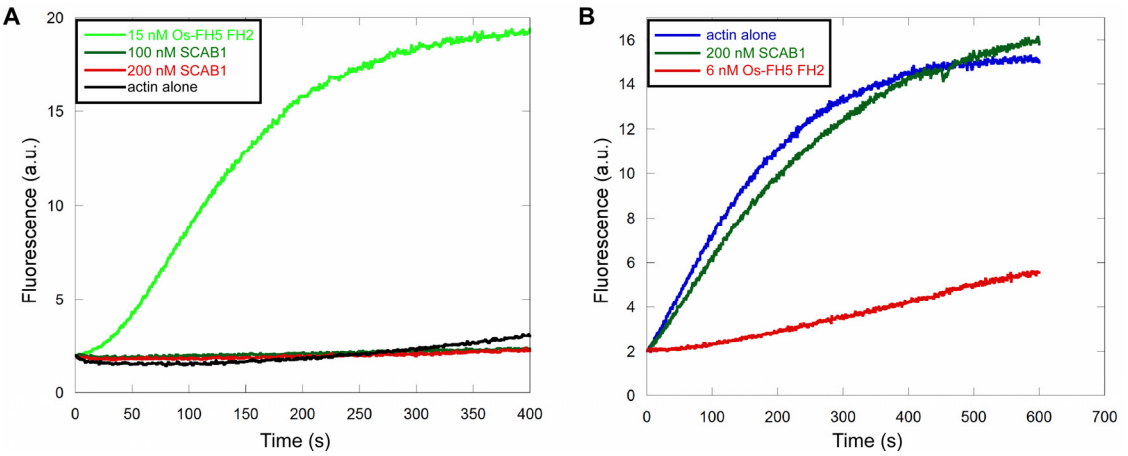

Supplemental Figure 3. SCAB1 lacks nucleation or capping activity.
(A) Time course of actin polymerization in the presence of SCAB1 or Os-FH5 FH2 monitored by pyrene fluorescence. Actin nucleation assays were performed as described (Higgs et al., 1999). Proteins were incubated with G-actin (2 μM 5% pyrene-labeled) for 5 min at room temperature. After the addition of 1/10 volume of 10× KMEI buffer (100 mM imidazole, 500 mM KCl, 10 mM $MgCl_2$, and 10 mM EGTA, pH 7.0), pyrene fluorescence was monitored immediately using a QuantaMaster Luminescence QM 3 PH fluorometer (Photo Technology International). Os-FH5 FH2, which can nucleate actin assembly (Yang et al., 2011; Zhang et al., 2011), was used as a positive control. a.u., arbitrary units.
(B) Kinetics of actin filament barbed-end elongation in the presence of SCAB1 or Os-FH5 FH2. Actin elongation assays were performed as described (Michelot et al., 2005). Preformed actin filament seeds (0.8 μM) were incubated with 200 nM SCAB1 or 6 nM Os-FH5 FH2 at room temperature for 5 min. Pyrene fluorescence was monitored after the addition of 1.0 μM G-actin (10% pyrene-labeled) saturated with 4 μM human profilin I. a.u., arbitrary units. Os-FH5 FH2, which can cap the barbed end of actin filaments (Yang et al., 2011; Zhang et al., 2011), was used as a positive control. a.u., arbitrary units.

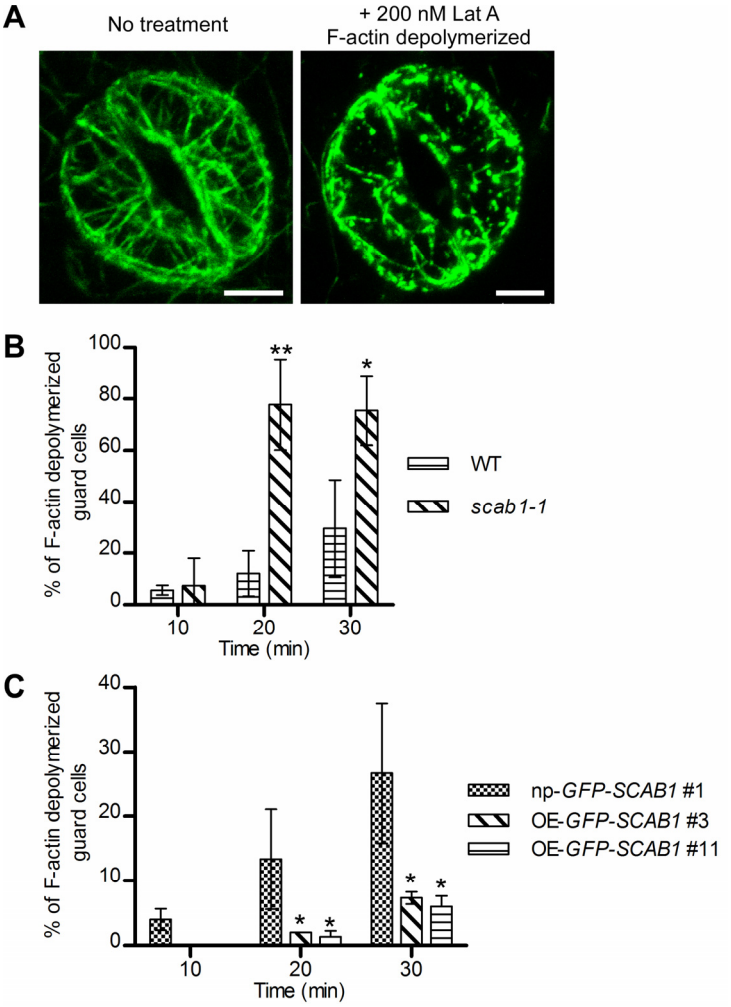

Supplemental Figure 4. SCAB1 delayed the Lat A-induced depolymerization of actin filaments in guard cells.

(A) Typical organization of actin filaments in guard cells from *35S:GFP-fABD2-GFP* transgenic plants without (left column) or with (right column) Lat A treatment. Scale bars, 5 μm.

(B) Percentage of guard cells from WT and *scab1-1* mutant plants with depolymerized actin filaments after Lat A treatment. The actin pattern shown in the right column in (A) was defined as depolymerized. Significant differences were observed between WT and *scab1-1* after 20 and 30 min of treatment (*$p < 0.05$, **$p < 0.01$, one-way ANOVA; post hoc: Tukey HSD). At least 50 guard cells were analyzed in each experiment (means ± SD, $n = 3$).

(C) Percentage of guard cells from np-*GFP-SCAB1* #1 and OE-*GFP-SCAB1* plants with depolymerized actin filaments after Lat A treatment. Significant differences were observed between np-*GFP-SCAB1* #1 and OE-*GFP-SCAB1*

plants after 20 and 30 min of treatment (*$p < 0.05$, one-way ANOVA; post hoc: Tukey HSD). At least 50 guard cells were analyzed in each experiment (means ± SD, $n = 3$). F-actin depolymerization in guard cells was assessed using cotyledons from 6-day-old transgenic seedlings harboring *35S:GFP-fABD2-GFP*. The seedlings were treated with 200 nM Lat A for 10, 20, or 30 min. The status of the actin filaments was determined using a Zeiss LSM510 Meta confocal microscope with a Plan-Apochromat 63×/1.4 oil objective. Those cells exhibiting dot-like GFP fluorescence were considered to be F-actin-depolymerized.

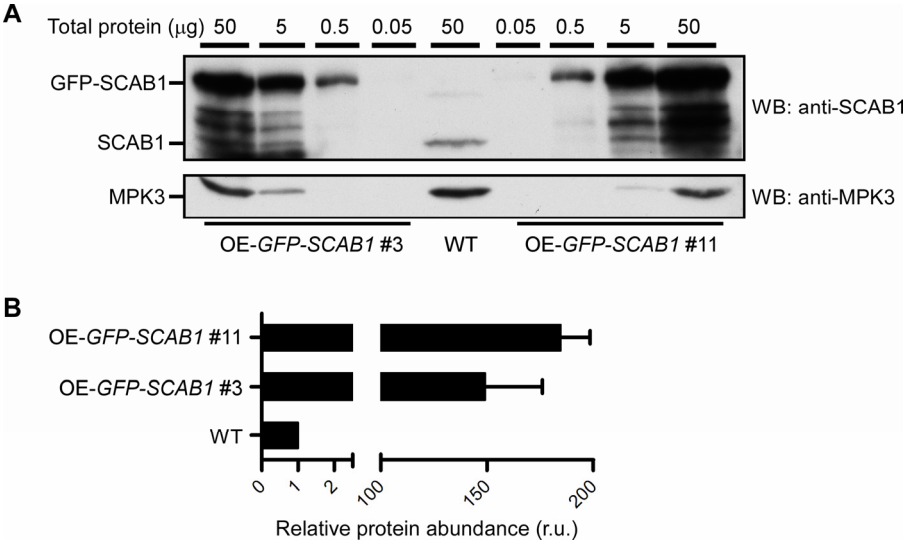

Supplemental Figure 5. Level of SCAB1 protein in *SCAB1* overexpressing plants.

(A) Immunoblot analysis of 50 μg of total soluble protein extracted from 1-day-old WT and *GFP-SCAB1* overexpression plants with anti-SCAB1 or -MPK3 (loading control) antibodies.

(B) The experiments described in **(A)** were repeated 3 times. The amount of SCAB1 was determined by densitometry. The SCAB1 protein level in WT was arbitrarily set to 1. r.u., relative unit. The data given are the means ± SD.

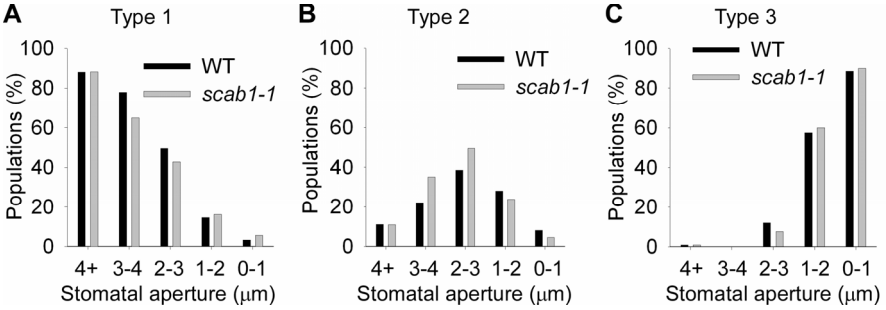

Supplemental Figure 6. Histograms showing the stomatal apertures with actin organization in guard cells from WT and *scab1-1* plants.
Confocal images of guard cells in rosette leaves from *Pro35S:GFP-fABD2-GFP* transgenic plants in a WT and *scab1-1* background were obtained following 20 μM ABA treatment. Actin organization was classified into 3 groups. Representative images of type 1 'radial array', type 2 'random meshwork', and type 3 'longitudinal array' are shown in Figure 8A-C, respectively. At the indicated stage of stomatal opening, the guard cells were classified into 3 groups: type 1 **(A)**, type 2 **(B)**, and type 3 **(C)**. Population distributions were examined in 985 (WT) and 964 (*scab1-1*) independent guard cells.

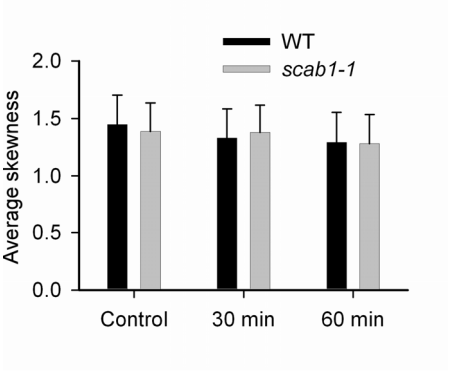

Supplemental Figure 7. SCAB1 does not alter skewness in guard cells.
Confocal images of guard cells in rosette leaves from *Pro35S:GFP-fABD2-GFP* transgenic plants in a WT or *scab1-1* background were obtained at the indicated times after 20 μM ABA treatment. The micrographs were analyzed using ImageJ with the plugins Hig Skewness and KbiPlugins (available at http://hasezawa.ib.k.u-tokyo.ac.jp/zp/Kbi/HigStomata). The data given are the means ± SD of 100-120 independent pairs of guard cells.

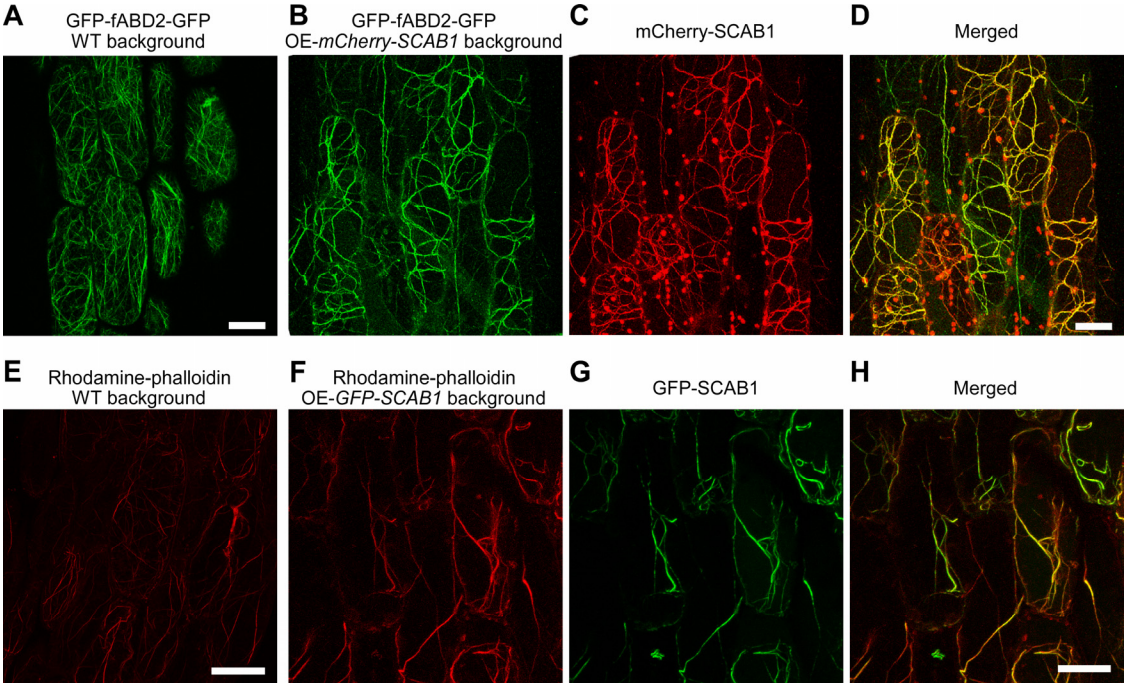

Supplemental Figure 8. SCAB1 bundles MFs in *vivo*.
(A-B) Typical GFP-fABD2-GFP images in hypocotyl epidermal cells taken from transgenic plants in a WT background **(A)** and in an *mCherry-SCAB1* overexpression background **(B)**. Note that fABD2 in **(B)** has fewer actin filaments or bundles and more thick actin bundles compared with that in **(A)**. About 83% of the cells in the WT background showed a pattern similar to that in **(A)**, whereas 93% of the cells in the OE-*mCherry-SCAB1* background showed a pattern similar to that in **(B)**. The dots in **(C)** are from chlorophyll autofluorescence. About 100 cells in 4 independent experiments with at least 3 individual transgenic lines per background were counted.
(C) The corresponding mCherry channel of **(B)**.
(D) Merged image of **(B)** and **(C)**.
(E-H) Rhodamine-phalloidin-stained actin filaments stained in hypocotyl epidermal cells of transgenic plants in a WT background **(E)** and in a *GFP-SCAB1* overexpression background **(F)**. The MFs in **(F)** have thicker actin bundles compared with those in **(E)**. Some local differences in the merged image are due to differences in GFP-SCAB1 expression level and rhodamine-phalloidin staining level.
(G) The corresponding GFP channel of **(F)**.
(H) Merged image of **(F)** and **(G)**.
Scale bars, 20 μm.

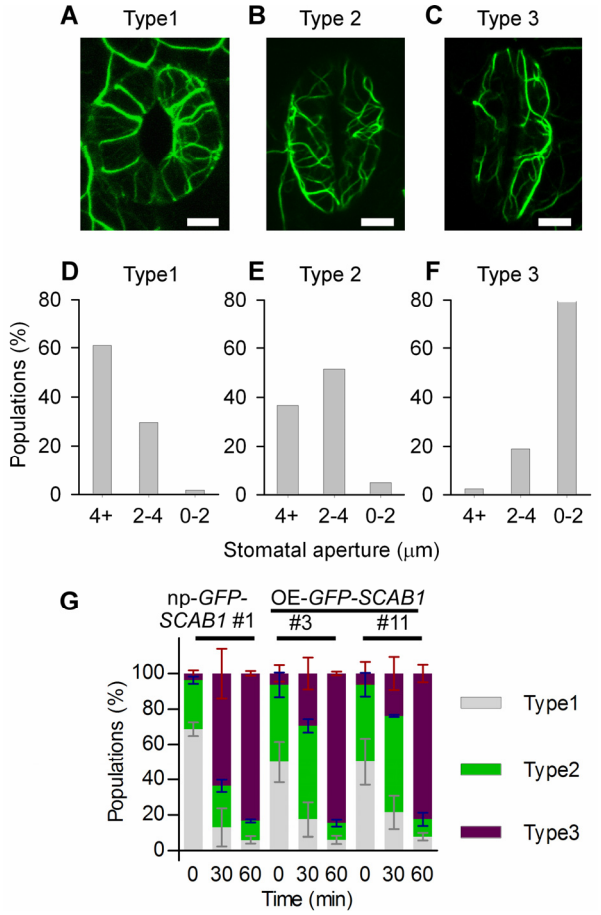

Supplemental Figure 9. Overexpression of SCAB1 delays GFP-SCAB1-labeled actin reorganization during stomatal closure.

(A-C) Confocal images of guard cells in rosette leaves from *GFP-SCAB1* transgenic plants were obtained following 20 μM ABA treatment. SCAB1 localization was classified into 3 groups. Representative images of type 1 'radial array' **(A)**, type 2 'random meshwork' **(B)**, and type 3 'longitudinal array' **(C)** are shown. Bars, 5 μm.

(D-F) At the indicated stage of stomatal opening, guard cells were classified into 3 groups according to the SCAB1 patterns in **(A-C)**. Stomatal aperture was measured using LSM Image Browser software. The population distributions were examined in 617 independent guard cells.

(G) Histograms showing the GFP-SCAB1-labeled MF organization in guard cells from np-*GFP-SCAB1* #1 and OE-*GFP-SCAB1* plants at the indicated times after ABA treatment. The data represent the mean ± SD of 3 independent experiments; at least 100 guard cells per line were measured at the indicated times.

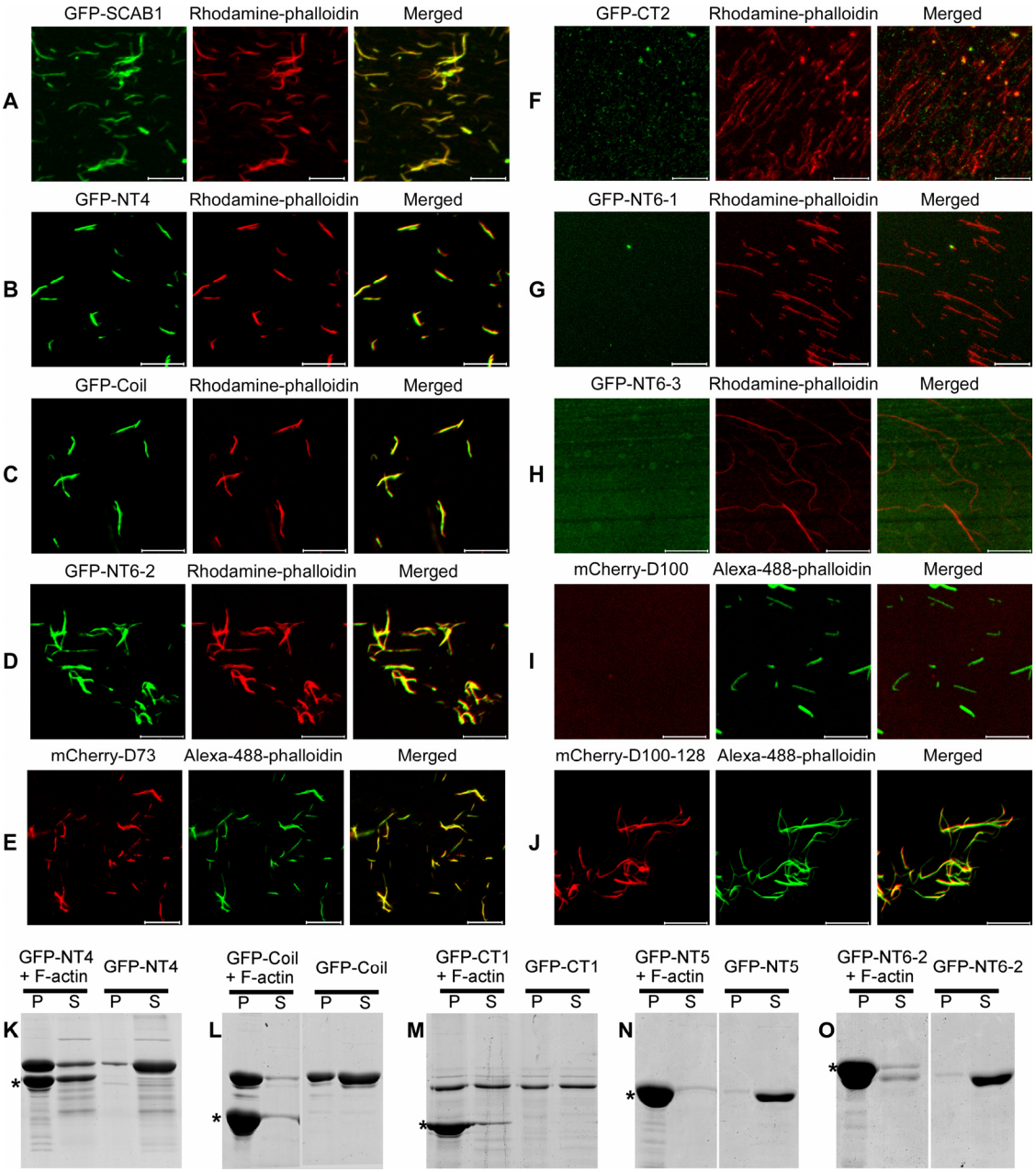

Supplemental Figure 10. Identification of the actin-binding domain of SCAB1.

(A-J) Rhodamine-phalloidin- **(A-D** and **F-H)** or Alexa-488-phalloidin-stained **(E**, **I**, and **J)** actin filaments were incubated with GFP-tagged SCAB1 **(A)**, NT4 **(B)**, Coil **(C)**, NT6-2 **(D)**, CT2 **(F)**, NT6-1 **(G)**, or NT6-3 **(H)**, and mCherry-tagged D73 **(E)**, D100 **(I)**, or D100-128 **(J)**. Left panel: GFP or mCherry labeled SCAB1 truncated proteins; middle panel: actin filaments stained with rhodamine- or

Alexa-488-phalloidin; right panel: merged images. Bars, 10 μm.
(K-O) High-speed cosedimentation assays of GFP-NT4 **(K)**, GFP-Coil **(L)**, GFP-CT1 **(M)**, GFP-NT5 **(N)**, and GFP-NT6-2 **(O)** in the presence or absence of MFs. After centrifugation at 150,000 x *g*, the proteins in the supernatant (S) and pellet (P) were resolved by SDS-PAGE. Asterisks represent actin.

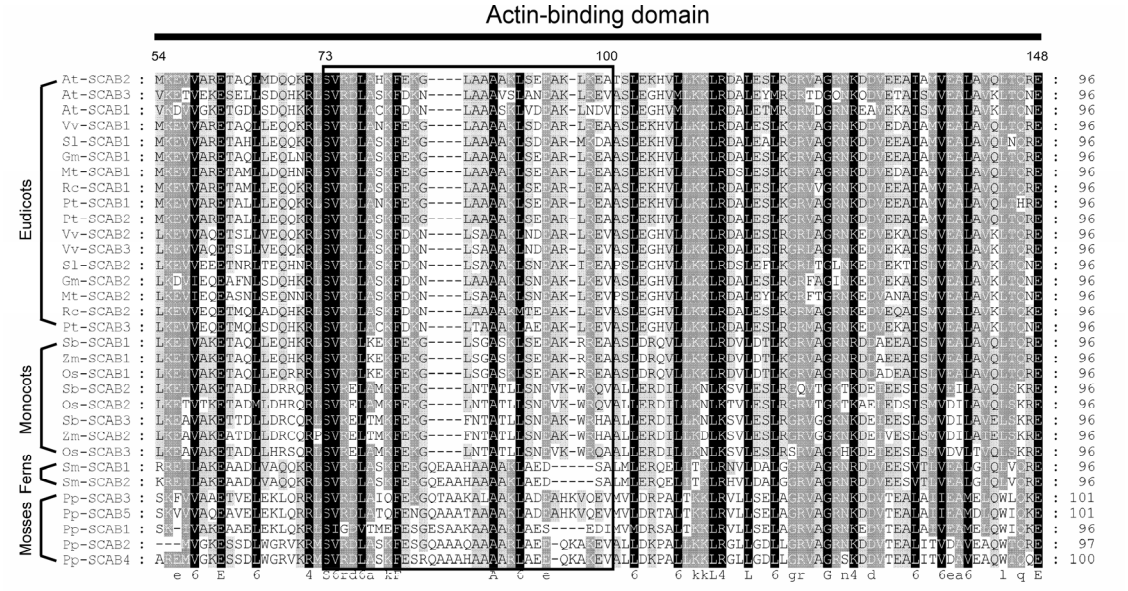

Supplemental Figure 11. Alignment of the actin-binding domains from SCAB1 homologs.

SCAB1 homologs from *Arabidopsis*, bean, alfalfa, grape, poplar, castor, tomato, rice, maize, sorghum, *Selaginella*, and *Physcomitrella* (Supplemental Table 1 online) were aligned using ClustalX 2.0.5 (Larkin et al., 2007) with the default settings. The conserved actin-binding region was selected and viewed using GeneDoc software (http://www.nrbsc.org/gfx/genedoc/). The residues indicated by the rectangular box (corresponding to residues 73-100 of SCAB1) were critical for actin binding.

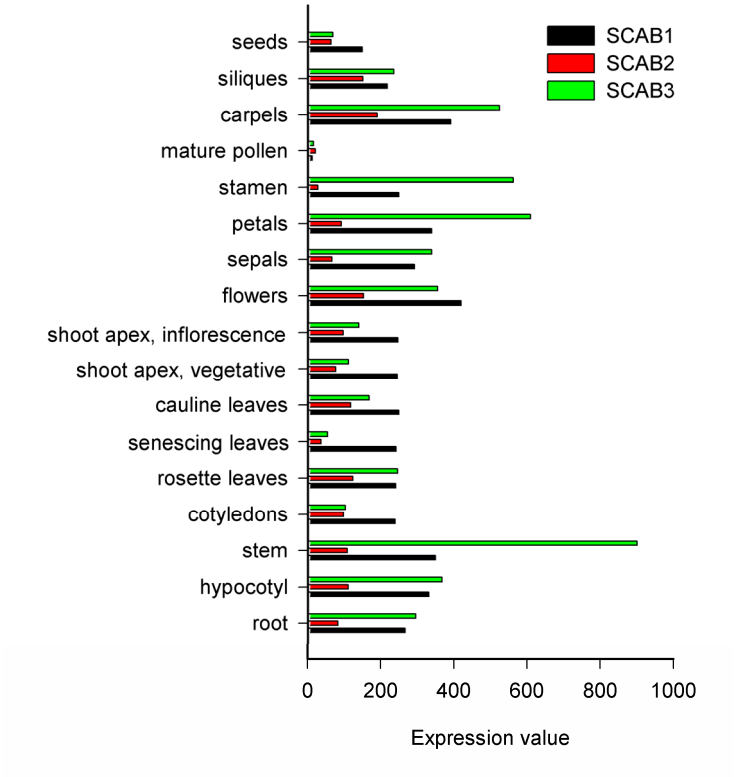

Supplemental Figure 12. Expression of *SCAB1* and its homologous genes in *Arabidopsis*.

Microarray analysis of the expression of *SCAB1* and its homologs in different organs using data from AtGeneExpress (Schmid et al., 2005).

Supplemental Table 1. Accession number of proteins with sequence similarity to SCAB1 (E-value < 1e-90).

Species	Protein ID	Accession number	Gene Locus
Arabidopsis thaliana	AtSCAB1	O48791	At2g26770
	AtSCAB2	Q8GX05	At3g56480
	AtSCAB3		At3g56480
Glycine max	GmSCAB1	C6TC02	
	GmSCAB2	C6TEU5	
Medicago truncatula	MtSCAB1		Medtr5g095960
	MtSCAB2		Medtr7g106120
Populus trichocarpa	PtSCAB1	B9HNJ6	POPTRDRAFT_804415
	PtSCAB2	B9GFS8	POPTRDRAFT_752371
	PtSCAB3	B9H8S2	POPTRDRAFT_818999
	PtSCAB4	B9IHM8	POPTRDRAFT_734721
Ricinus communis	RcSCAB1	B9SB74	RCOM_0785850
	RcSCAB2	B9RU60	RCOM_1632320
Solanum lycopersicum	SlSCAB1		SL1.00sc05103_116.1.1
	SlSCAB2		SL1.00sc00141_157.1.1
Vitis vinifera	VvSCAB1	D7T1E3	VIT_00037402001
	VvSCAB2	D7TQT9	VIT_00025779001
	VvSCAB3	A5ALR3	VITISV_039755
Oryza sativa	OsSCAB1	Q0JIF1	Os01g0805700
	OsSCAB2	Q10KZ6	Os03g0364500
	OsSCAB3	Q7XHY6	Os07g0642800
Sorghum bicolor	SbSCAB1	C5XMJ3	Sb03g037470
	SbSCAB2	C5WYR7	Sb01g034550
	SbSCAB3	C5X3Y5	Sb02g040980
Zea mays	ZmSCAB1	B4FKU4	Zm.5950.
	ZmSCAB2	B4FKT7	Zm.17411.
Selaginella moellendorffii	SmSCAB1	D8SYV7	SELMODRAFT_128387
	SmSCAB2	D8S730	SELMODRAFT_110449
Physcomitrella patens	PpSCAB1	A9RK58	PHYPADRAFT_115719
	PpSCAB2	A9SLZ6	PHYPADRAFT_213766
	PpSCAB3	A9TJ68	PHYPADRAFT_146374
	PpSCAB4	A9TGG1	PHYPADRAFT_145201
	PpSCAB5	A9S5Y9	PHYPADRAFT_124545

Supplemental Table 2. Primers used in this study.

Primer name	Sequence
pSKI015 RB	5'-TAATACGACTCACTATAGGGC-3'
pCSA110 LB1	5'-GCCTTTTCAGAAATGGATAAATAGCCTTGCTTCC-3'
pCSA110 LB3	5'-TAGCATCTGAATTTCATAACCAATCTCGATACAC-3'
scab1-1 F	5'-GTGGCAGGTAGAAACAAGGATG-3'
scab1-1 R	5'-GAGCAAGGTCTAACTCGCAAAC-3'
scab1-2 F	5'-TCGCTGAGTCAACTGAAC-3'
scab1-2 R	5'-GTCGGATCCATGACAAGGGTTACACGCGATTTTC-3'
SCAB1 F	5'-ATGAGCTTCGAGCACTAAGAAATCAGC-3'
SCAB1 R	5'-GAGCAAGGTCTAACTCGCAAAC-3'
EF1α F	5'-TGAGCACGCTCTTCTTGCTTTCA-3'
EF1α R	5'-GGTGGTGGCATCCATCTTGTTACA-3'
SCAB1 CDSF	5'-GTCGGATCCATGACAAGGGTTACACGCGATTTTC-3'
SCAB1 CDSR	5'-GCTGAATTCTCAAGGGCTTTGACCCGTCTC-3'
*SCAB1Pro Pst*IF	5'-AGCTGCAGTGGGAACTTATAGTTTATCCG-3'
*SCAB1Pro Bam*HIR	5'-GTCGGATCCTGTATCTGTTTATAAACAAAACC-3'
*GFP Bam*HIF	5'-AAGGATCCATGGTGAGCAAGGGCGAG-3'
*GFP Bam*HIR	5'-ATGGATCCCTTGTACAGCTCGTCCATG-3'

Supplemental Table 3. Primers used for plasmid constructions.

Plasmids	Forward primers	Reverse primers
pCAMBIA1205-GFP-Coil	5’-TCGGATCCATGAAAGAGGTTGTTGCG-3’	5’-CTGAATTCTCACTTTCTGCACATTGCGAG-3’
pCAMBIA1205-GFP-NT4	5’-GTCGGATCCATGACAAGGGTTACACGCGATTTTC-3’	5’-CTGAATTCTCATCGCTGAGTCAACTGAAC-3’
pCAMBIA1205-GFP-NT5	5’-TCGGATCCATGAAAGAGGTTGTTGCG-3’	5’-CTGAATTCTCATCGCTGAGTCAACTGAAC-3’
pCAMBIA1205-GFP-NT6-1	5’-TCGGATCCATGGTTCGTGACCTCGCTC-3’	5’-CTGAATTCTCACTTGTTTCTACCTGCCAC-3’
pCAMBIA1205-GFP-NT6-2	5’-TCGGATCCATGGTTCGTGACCTCGCTC-3’	5’-CTGAATTCTCATCGCTGAGTCAACTGAAC-3’
pCAMBIA1205-GFP-NT6-3	5’-TCGGATCCATGAAAGAGGTTGTTGCG-3’	5’-CTGAATTCTCACTTGTTTCTACCTGCCAC-3’
pCAMBIA1205-GFP-CT1	5’-TAGGATCCATGGATATGGAATATGAGCTTC-3’	5’-GCTGAATTCTCAAGGGCTTTGACCCGTCTC-3’
pCAMBIA1205-GFP-CT2	5’-TAGGATCCAGCGAGGAAAATATATCCCTTG-3’	5’-GCTGAATTCTCAAGGGCTTTGACCCGTCTC-3’
pCAMBIA1205-mCherry-D73	5’-TCGGATCCGTTCGTGACCTCGCTC-3’	5’-GCTGAATTCTCAAGGGCTTTGACCCGTCTC-3’
pCAMBIA1205-mCherry-D100	5’-TCGGATCCATGACTTCGTTGGAGAAAC-3’	5’-GCTGAATTCTCAAGGGCTTTGACCCGTCTC-3’
pCAMBIA1205-mCherry-D73-100	5’-GTCGGATCCATGACAAGGGTTACACGCGATTTTC-3’	5’-CATGTTTCTCCAACGAAGTAGACAAACGTTTCTGCTG-3’
	5’-CAGCAGAAACGTTTGTCTACTTCGTTGGAGAAACATG-3’	5’-GCTGAATTCTCAAGGGCTTTGACCCGTCTC-3’
pCAMBIA1205-mCherry-D100-128	5’-GTCGGATCCATGACAAGGGTTACACGCGATTTTC-3’	5’-ATGGCTTCCTCTACATCATCTGCTTCTTTGAGTTTTGCCT-3’
	5’-AGGCAAAACTCAAAGAAGCAGATGATGTAGAGGAAGCCAT-3’	5’-GCTGAATTCTCAAGGGCTTTGACCCGTCTC-3’